J. Am. Chem. Soc. **1986**, *108*, 2582–2588

Crystal and Molecular Structure of the Charge Transfer Salt of Decamethylferrocenium and Tricyanomethanide: $[Fe(C_5Me_5)_2]^{+}\cdot[C(CN)_3]^-$. The Electronic Structure and Spectra of $[C(CN)_3]^-$

David A. Dixon,* Joseph C. Calabrese, and Joel S. Miller*

Contribution No. 3807, Central Research and Development Department, E. I. du Pont de Nemours & Co., Wilmington, Delaware 19898.

Received June 28, 1985

Abstract: The reaction of decamethylferrocenium tetrafluoroborate, $[Fe(C_5Me_5)_2]^{+}\cdot[BF_4]^-$, and potassium tricyanomethanide, $K[C(CN)_3]$, leads to the isolation of $[Fe(C_5Me_5)_2]^{+}\cdot[C(CN)_3]^-$. The crystal and molecular structure of this substance has been determined by single-crystal X-ray analysis at −100 °C; the green complex crystallizes as needles in the orthorhombic *Pma*2 space group (No. 28) [a = 22.375 (4) Å, b = 21.331 (2) Å, c = 9.420 (3) Å, V = 4496.0 Å^3, and Z = 8]. There are no cation–anion chains within the structure, and the closest Fe(III)–Fe(III) distance is 8.03 Å. The cation is ordered and shows no unusual bond lengths or angles. The anion structure possesses approximate D_{3h} local symmetry with all C—C and C≡N distances ranging from 1.367 (18) to 1.430 (10) Å and 1.143 (10) to 1.192 (20) Å, respectively. This structure is comprised of three independent $[Fe(C_5Me_5)_2]^{+}\cdot$ cations and four independent $[C(CN)_3]^-$ anions per unit cell with all cations and anions being essentially equivalent to themselves. There is no evidence for a structure with C_{2v} symmetry corresponding to the $[(NC)_2C{=}C{=}N]^-$ resonance form. The $[C(CN)_3]^-$ ion has been characterized by a variety of spectroscopic techniques. The infrared and Raman spectra confirm the D_{3h} structure. Two new weak transitions in the UV–visible spectrum at 42 550 cm^{-1} ($\epsilon \sim$ 1000 M^{-1} cm^{-1}) and 36 360 cm^{-1} ($\epsilon \sim$ 700 M^{-1} cm^{-1}) have been observed and are assigned to the forbidden $^1A_1 \rightarrow {}^1E''$ (HOMO → LUMO) transition split by a Jahn–Teller distortion. The electronic structures of $[C(CN)_3]^-$ and $[C(CN)_3]^+$ have been determined by ab initio molecular orbital theory with the 3-21G basis set and with a double-ζ basis set augmented by a set of d polarization functions at the central carbon. The geometries were determined with both basis sets. The force field was determined with the 3-21G basis set and the frequencies are compared to the experimental values. These results confirm the D_{3h} structure of $[C(CN)_3]^-$. Various charge distributions are presented and discussed in terms of classical resonance structures.

Since the observation of metamagnetism[1] for the one-dimensional phase of $[Fe(C_5Me_5)_2]^{+}\cdot(TCNQ)^{-}\cdot$ (TCNQ = 7,7,8,8-tetracyano-*p*-quinodimethane) as well the observation of a multitude of other magnetic properties for various phases of polycyanoanionic acceptors[2-4] and decamethylferrocene, we have undertaken the systematic study of the structure–function relationship between planar strong acceptors and metallocenium donors. Previously we have reported on the three phases of decamethylferrocene and TCNQ[1,5,6] as well as the 1:2 salt of trimethyleneferrocene and TCNQ,[7] the 1:1 salt with DDQ[3] (DDQ = 2,3-dicyano-5,6-dichloro-*p*-benzoquinone) and the 1:2 salt of 1,1′-dimethylferrocene and TCNQ.[8] Recently, we have reported that the 1:1 salt of $Fe(C_5Me_5)_2$ and TCNE (TCNE = tetracyanoethylene) exhibits a ferromagnetic ground state.[4] The structures and Mössbauer and the magnetic susceptibility of the $[TCNE]^{-}\cdot$ and $[C_3(CN)_5]^-$ salts of $[Fe(C_5Me_5)_2]^{+}\cdot$ have been determined. In order to get a better systematic handle on this class of substances, particularly from a theoretical perspective, we have prepared $[Fe(C_5Me_5)_2]^{+}\cdot[C(CN)_3]^-$ and studied its physical properties. We are particularly interested in this compound as it allows comparison with other percyano anions and also provides a closed shell model compound with which to compare other cyano radical anion complexes.

We are further interested in the nature of the $[C(CN)_3]^-$ anion. There have been a number of prior experimental studies[9-17] of this ion which suggest that it has a D_{3h} structure; however, there is also some evidence that a C_{2v} distortion can occur.[18] Our study with a diffuse cation should minimize a number of crystal interactions. Furthermore, since there have not been any good theoretical studies of the electronic structure of $[C(CN)_3]^-$, we have performed ab initio molecular orbital calculations with reasonable basis sets in order to better understand $[C(CN)_3]^-$. Additionally, due to recent attempts to synthesize[12] $[C(CN)_3]^+$, we have also studied this cation theoretically.

Experimental Section

Preparation of $[Fe(C_5Me_5)_2]^{+}\cdot[C(CN)_3]^-$. To a filtered acetonitrile solution containing 250 mg (1.94 mmol) of $K[C(CN)_3]$ (Alfa) was added 720 mg (1.75 mmol) of $[Fe(C_5Me_5)_2]^{+}\cdot[BF_4]^-$ dissolved in acetonitrile. After 2 h the solvent (8 mL) was removed via a rotary evaporator and the green product was redissolved in methylene chloride and the byproduct extracted three times with 10 mL of distilled water in a sepratory funnel. The product was subsequently recrystallized from acetonitrile (yield 110 mg, 0.26 mmol, 15%). Anal. Calcd for $C_{24}H_{30}N_3Fe$: C, 68.76; H, 7.21; N, 10.02. Found: C, 68.64; H, 6.69; N, 9.88.

The PPN (PNN = bis(triphenylphosphine)iminium) salt of $[C(CN)_3]^-$ was prepared from reaction of bis(triphenylphosphine)iminium

---

[1] Candela, G. A.; Swartzendruber, L.; Miller, J. S.; Rice, M. J. *J. Am. Chem. Soc.* **1979**, *101*, 2755.

[2] Miller, J. S.; Krusic, P. J.; Calabrese, J. C.; Epstein, A. J. *Mol. Cryst. Liq. Cryst.* **1985**, *120*, 27.

[3] Gerbert, E.; Reis, A. H., Jr.; Miller, J. S.; Rommelmann, H.; Epstein, A. J. *J. Am. Chem. Soc.* **1982**, *104*, 4403.

[4] Miller, J. S.; Calabrese, J. C.; Epstein, A. J.; Reiff, W. M., Zhang, J. H., submitted for publication.

[5] Miller, J. S.; Reiff, W. M.; Zhang, J. H.; Dixon, D. A.; Preston, L. D.; Reis, A. H., Jr.; Gebert, E.; Extine, M.; Troup, J.; Epstein, A. J., in preparation.

[6] Miller, J. S.; Reis, A. H., Jr.; Gebert, E.; Ritsko, J. J.; Salaneck, W. R.; Kovnat, L.; Cape, T. W.; Van Duyne, R. P. *J. Am. Chem. Soc.* **1979**, *101*, 7111.

[7] Willi, C.; Reis, A. H., Jr.; Gebert, E.; Miller, J. S. *Inorg. Chem.* **1981**, *20*, 313, 318.

[8] Wilson, S. R.; Corvan, P. J.; Seiders, R. P.; Hodgson, D. S.; Brookhart, M.; Hatfield, W. E.; Miller, J. S.; Reis, A. H., Jr.; Rogan, P. K.; Gebert, E.; Epstein, A. J. "Molecular Metals"; Hatfield, W. E., Ed.; Plenum Publishing Corp.: New York, 1979; p 407.

[9] Enemark, J. H.; Holm, R. H. *Inorg. Chem.* **1964**, *3*, 1516.

[10] Boyd, R. H. *J. Phys. Chem.* **1963**, *67*, 737.

[11] Miller, F. A.; Baer, W. K. *Spectrochem. Acta* **1963**, *19*, 73.

[12] Beaumont, R. C.; Aspin, K. B.; Demas, T. J.; Hoggatt, J. H.; Potter, G. E. *Inorg. Chem. Acta* **1984**, *84*, 141.

[13] Long, D. A.; Carrington, R. A. G.; Gravenor, R. B. *Nature* (*London*) **1962**, *196*, 371.

[14] Andersen, P.; Kewe, B. *Nature* (*London*) **1963**, *200*, 464.

[15] Witt, J. R.; Britton, D. *Acta. Crystallogr.* **1971**, *B27*, 1835.

[16] Britton, D.; Chow, Y. M. *Acta. Crystallogr.* **1983**, *C39*, 1539.

[17] Desiderato, R.; Sass, R. L. *Acta. Crystallogr.* **1965**, *18*, 1.

[18] Konnert, J.; Britton, D. *Inorg. Chem.* **1966**, *5*, 1193.

0002-7863/86/1508-2582$01.50/0

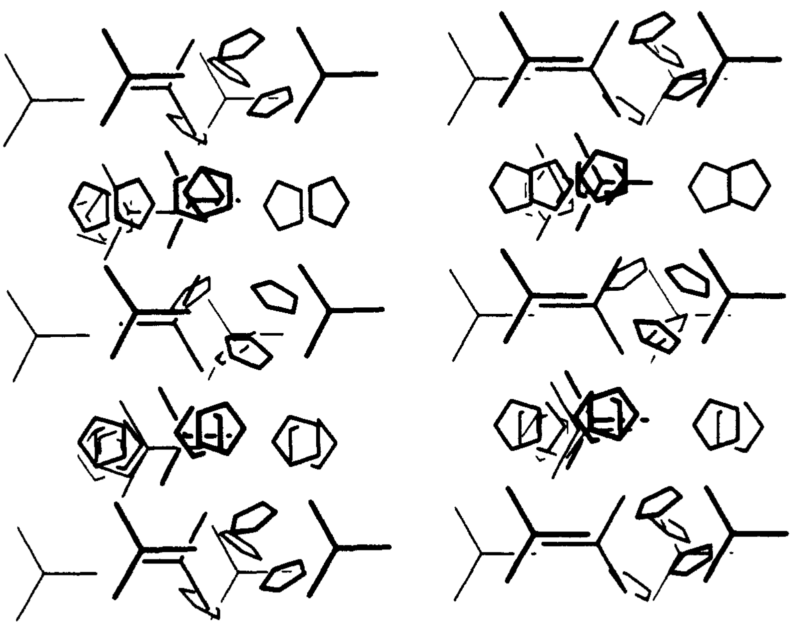

Figure 1. Stereoview down the *b* axis for a unit cell of $[FeC_5Me_5)_2]^{+}\cdot[C(CN)_3]^-$.

chloride (Alfa) (840 mg, 1.47 mmol) and 190 mg (1.47 mmol) of $K[C(CN)_3]$ dissolved in methanol. The white solid which precipitates was filtered off and washed with water and vacuum dried (yield 720 mg (1.14 mmol; 78%); mp 145–146 °C). Anal. Calcd for $C_{40}H_{30}N_4P_2$: C, 76.42; H, 4.81; N, 8.91. Found: C, 76.38; H, 4.96; N, 8.87. The tetra(*n*-butyl)ammonium salt was prepared from $[n\text{-}Bu_4N]^+[BF_4]^-$ and $K[C(CN)_3]$ in 10 mL of methanol. The complex was extracted with Et_2O after drying over $MgSO_4$ and vacuum dried (yield 55%). Anal. Calcd for $C_{20}H_{36}N_3$: C, 72.24; H, 10.91; N, 16.85. Found: C, 72.21; H, 11.08; N, 16.36.

The crystal structure data were obtained from a green irregular cut block of dimensions 0.30 × 0.19 × 0.30 mm. The space group is orthorhombic, *Pma*2 (No. 28) with $a = 22.375$ (4) Å, $b = 21.331$ (2) Å, and $c = 9.420$ (3) Å as determined from 24 reflections. The volume of the unit cell is 4496.0 Å,³ giving a density of 1.230 g/cm³ with $Z = 8$.

The data were collected at −100 °C on a Syntex R3 diffractometer equipped with a graphite monochromator; Mo Kα radiation ($\lambda = 0.7107$ Å) was used. The 5872 data points were collected (*acb*) over the range 4.1° ≤ 2θ ≤ 55.0°. The maximum *h*, *k*, *l* = 29, 12, 27 for data octants = +++. The ω scan method was employed with scan width = 1.00° ω and scan speed = 2.00–9.80°/min. A typical half-height peak width was 0.26 ω. Three standards were collected 32 times and the data were adjusted for a 3% decrease in intensity. There was a 4.7% variation in azimuthal scan. The intensities were corrected for absorption (DIFABS).[19a] There were 3492 unique reflections with $I \geq 2.0\sigma(I)$.

The structure was successfully solved by direct methods (MULTAN)[19b] with space group *Pma*2. Refinement was by full-matrix least squares on *F*. Scattering factors were from standard tables,[20] including anomalous terms for Fe. The weights are proportional to $[\sigma^2(I) + 0.0009I^2]^{-1/2}$. A total of 531 parameters were refined with all non-hydrogen atoms refined anisotropically and all hydrogen atoms fixed. The final value for *R* is 0.060 with $R_w = 0.048$. The error of fit is 1.21 with a maximum $\Delta/\sigma = 0.13$ (all $l = 12$ reflections were omitted due to background imbalance). The enantiomorph chosen corresponds to the lowest *R* value. The largest residual density of 0.61 e⁻/Å³ is located in a small cavity 2.1 Å from the nitrogen atom in one of the tricyanomethide ions.

Spectroscopic Measurements. The infrared spectra were recorded on a Nicolet 7199 Fourier Transform spectrometer. The Raman spectra were recorded on a J-Y Raman Microprobe. The UV-visible spectra were recorded on a Cary 2390 spectrometer. Zero-field Mössbauer were determined with a conventional constant acceleration spectrometer with a 150 mCurie ^{57}Co source which is electroplated onto the surface and annealed into the body of a 6 μm thick foil of high purity rhodium. Further details may be found in the literature.[21]

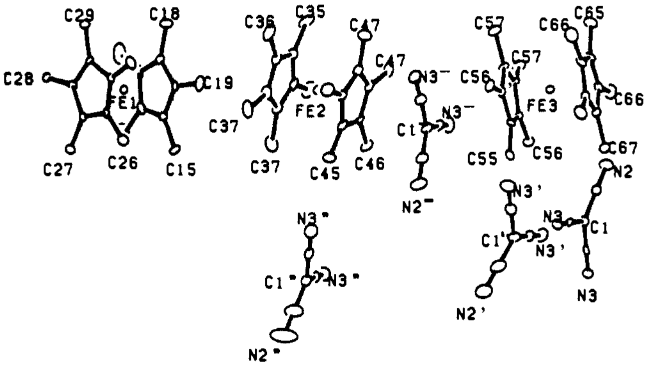

Figure 2. Crystallographically inequivalent cations and anions showing the atom labeling. The ring carbons are labeled as the methyl carbon label minus five.

Molecular Orbital Calculations. The molecular orbital calculations were done with the HONDO program[22] on an IBM 3083 computer. Geometries were gradient optimized[23] with both the 3-21G basis set[24] and a double-ζ basis set augmented by polarization functions on the central carbon (DZ+D$_C$).[25] The vibrational frequencies for the anion $[C(CN)_3]^-$ and the cation $[C(CN)_3]^+$ were determined by numerical differentiation of the gradient with the 3-21G basis set.

Results and Discussion

Crystal Structure. The green complex crystallizes with eight ion pairs per unit cell. One $[Fe(C_5Me_5)_2]^{+}\cdot$ cation exists in a general position, and two half-cations are on the mirror at $^1/_4$ on *x*. The asymmetric unit also has four half-tricyanomethanide anions, two on different twofolds and two on different mirrors. The unit cell is shown in Figure 1 and a schematic with atom labels is given in Figure 2. The refined coordinates are given in Table I, anisotropic thermal parameters are presented in Table II, and the intraatomic distances and angles are listed in Tables III and IV, respectively. The cations and anions are isolated from each other and no unusually short interactions exist. The closest Fe–Fe distance is 8.03 Å, and neither a linear chain nor layer structural

---

(19) (a) Walker, N.; Stuart, D. *Acta Crystallogr.* **1983**, *A39*, 158. (b) Main, P.; Lessinger, L.; Woolfson, M. M. Germain, G.; Declarq, J. P., MULTAN, York, England, and Louvain-la-Neuve, Belgium, 1978.

(20) "International Tables for X-ray Crystallography"; Kynoch Press: Birmingham, England, 1974; Vol. IV.

(21) Chen, C.; Reiff, W. M. *Inorg. Chem.* **1977**, *16*, 2097.

(22) (a) Dupuis, M.; Rys, J.; King, H. F. *J. Chem. Phys.* **1976**, *65*, 111. (b) King, H. F.; Dupuis, M.; Rys, J. *National Resource for Computer Chemistry Software Catalog*, Vol. 1, Program QHO2 (HONDO), 1980.

(23) Pulay, P. In "Applications of Electronic Structure Theory"; Schaefer, H. F., III, Ed.; Plenum Press: New York, 1977, p 153.

(24) Binkley, J. S.; Pople, J. A.; Hehre, W. J. *J. Am. Chem. Soc.* **1980**, *102*, 939.

(25) Dunning, T. H., Jr.; Hay, P. J. In "Methods of Electronic Structure Theory"; Schaefer, H. F., III, Ed.; Plenum Press: New York, 1977; p 1.

Table I. Fractional Coordinates (×10000) and Isotropic Thermal Parameters for $[Fe(C_5Me_5)_2]^+[C(CN)_3]^-$

atom	x	y	z	B_{iso}, Å	atom	x	y	z	B_{iso}, Å
Fe(1)	153.5 (4)	−2574.5 (4)	6542.8	1.7 (1)′	C(66)	3650 (4)	5201 (5)	−1574 (12)	4.4 (3)′
Fe(2)	2500	22 (1)	2385 (2)	1.9 (1)′	C(67)	3224 (5)	5769 (4)	1399 (12)	4.4 (3)′
Fe(3)	2500	4599 (1)	6 (2)	1.6 (1)′	H(15)	1406	−1332	7670	3.5
N(2‘)	2500	2771 (6)	5614 (14)	4.7 (4)′	H(15′)	1131	−1815	8714	3.5
N(2)	5000	5000	510 (12)	4.2 (4)′	H(15″)	742	−1273	8119	3.5
N(2′)	7500	2256 (6)	5106 (17)	5.8 (5)′	H(16)	1909	−2858	6967	3.5
N(2″)	5000	0	11457 (19)	12.9 (9)′	H(16′)	1431	−3377	7156	3.5
N(3‘)	3503 (3)	2354 (3)	1735 (11)	4.4 (2)′	H(16″)	1460	−2822	8220	3.5
N(3)	4001 (3)	5031 (4)	4613 (7)	2.8 (2)′	H(17)	1242	−3309	3602	3.5
N(3′)	6498 (4)	2426 (4)	1103 (9)	4.8 (3)′	H(17′)	573	−3484	3777	3.5
N(3″)	4034 (4)	216 (4)	7389 (10)	4.2 (2)′	H(17″)	1032	−3673	4937	3.5
C(1‘)	2500	2480 (6)	3025 (13)	2.8 (3)′	H(18)	380	−2108	2449	3.5
C(1)	5000	5000	3261 (14)	2.5 (3)′	H(18′)	−217	−1993	3244	3.5
C(1′)	7500	2426 (6)	2403 (13)	3.2 (4)′	H(18″)	0	−2672	2958	3.5
C(1″)	5000	0	8747 (14)	3.5 (4)′	H(19)	445	−863	4934	3.5
C(2‘)	2500	2631 (7)	4435 (15)	3.1 (4)′	H(19′)	124	−980	6369	3.5
C(2)	5000	5000	1751 (15)	3.0 (4)′	H(19″)	−177	−1184	4958	3.5
C(2′)	7500	2344 (8)	3856 (18)	4.4 (5)′	H(25)	−1550	−2021	6897	3.5
C(2″)	5000	0	10240 (20)	7.0 (6)′	H(25′)	−1194	−1958	5491	3.5
C(3‘)	3040 (4)	2414 (4)	2293 (10)	3.0 (2)′	H(25″)	−1025	−1548	6792	3.5
C(3)	4443 (4)	5015 (4)	4004 (9)	2.2 (2)′	H(26)	−694	−1946	10016	3.5
C(3′)	6956 (4)	2424 (4)	1684 (12)	3.2 (2)′	H(26′)	−440	−1512	8838	3.5
C(3″)	4469 (4)	123 (4)	8004 (10)	2.7 (2)′	H(26″)	−8	−1890	9803	3.5
C(10)	873 (3)	−1964 (4)	6676 (10)	2.1 (2)′	H(27)	5	−3397	10394	3.5
C(11)	1086 (3)	−2577 (4)	6350 (10)	2.8 (2)′	H(27′)	445	−2854	10070	3.5
C(12)	816 (4)	−2766 (4)	5017 (10)	2.7 (2)′	H(27″)	548	−3511	9405	3.5
C(13)	449 (3)	−2260 (4)	4554 (8)	2.0 (2)′	H(28)	−342	−4343	7504	3.5
C(14)	492 (3)	−1774 (4)	5547 (9)	1.9 (2)′	H(28′)	317	−4125	7365	3.5
C(15)	1055 (5)	−1561 (5)	7896 (10)	4.3 (3)′	H(28″)	−88	−4162	6028	3.5
C(16)	1510 (4)	−2943 (5)	7257 (13)	5.5 (3)′	H(29)	−1319	−3474	5247	3.5
C(17)	932 (5)	−3358 (5)	4269 (12)	6.4 (4)′	H(29′)	−693	−3580	4583	3.5
C(18)	123 (5)	−2247 (5)	3182 (9)	4.2 (3)′	H(29″)	−1012	−2939	4404	3.5
C(19)	192 (4)	−1144 (4)	5445 (11)	3.6 (3)′	H(35)	2500	−1171	−797	3.5
C(20)	−745 (3)	−2446 (4)	6996 (8)	1.8 (2)′	H(35′)	2847	−541	−802	3.5
C(21)	−406 (3)	−2435 (3)	8288 (8)	1.8 (2)′	H(36)	3788	−1201	1272	3.5
C(22)	−115 (3)	−3028 (3)	8433 (8)	1.7 (2)′	H(36′)	3913	−569	2027	3.5
C(23)	−270 (3)	−3405 (4)	7250 (8)	1.6 (2)′	H(36″)	3681	−576	473	3.5
C(24)	−664 (3)	−3051 (3)	6358 (8)	1.6 (2)′	H(37)	3284	−1255	4891	3.5
C(25)	−1167 (3)	−1950 (4)	6500 (12)	3.1 (2)′	H(37′)	3033	−619	5429	3.5
C(26)	−385 (4)	−1899 (4)	9331 (9)	2.8 (2)′	H(37″)	3590	−632	4444	3.5
C(27)	260 (4)	−3216 (4)	9683 (9)	2.7 (2)′	H(45)	2500	1206	5643	3.5
C(28)	−76 (3)	−4071 (3)	7007 (8)	2.2 (2)′	H(45′)	2847	577	5633	3.5
C(29)	−949 (4)	−3284 (4)	5039 (10)	2.8 (2)′	H(46)	3766	1246	3486	3.5
C(30)	2500	−755 (6)	1065 (14)	2.8 (4)′	H(46′)	3891	643	2615	3.5
C(31)	3010 (4)	−767 (4)	1913 (12)	2.9 (3)′	H(46″)	3686	592	4186	3.5
C(32)	2814 (4)	−793 (4)	3351 (12)	3.3 (3)′	H(47)	3283	1316	−26	3.5
C(35)	2500	−742 (7)	−554 (18)	4.8 (5)′	H(47′)	3003	707	−635	3.5
C(36)	3656 (4)	−780 (4)	1406 (15)	4.7 (3)′	H(47″)	3564	670	332	3.5
C(37)	3211 (5)	−831 (5)	4646 (13)	5.4 (4)′	H(55)	2500	3970	3993	3.5
C(40)	2500	794 (5)	3767 (15)	2.6 (4)′	H(55′)	2153	4565	3526	3.5
C(41)	3018 (4)	810 (4)	2868 (10)	2.3 (2)′	H(56)	3779	3616	1993	3.5
C(42)	2816 (4)	837 (3)	1409 (12)	2.7 (3)′	H(56′)	3686	4332	2182	3.5
C(45)	2500	795 (6)	5334 (13)	3.6 (4)′	H(56″)	3895	4066	730	3.5
C(46)	3653 (4)	825 (4)	3342 (12)	3.7 (3)′	H(57)	3289	2988	−1199	3.5
C(47)	3207 (5)	887 (4)	144 (13)	4.3 (3)′	H(57′)	3588	3642	−1319	3.5
C(50)	2500	4092 (5)	1910 (11)	1.9 (3)′	H(57″)	3037	3481	−2250	3.5
C(51)	3010 (3)	3926 (4)	1086 (8)	2.0 (2)′	H(65)	2500	5215	−3970	3.5
C(52)	2813 (3)	3673 (4)	−231 (8)	1.9 (2)′	H(65′)	2153	4626	−3467	3.5
C(55)	2500	4328 (6)	3382 (14)	2.7 (4)′	H(66)	3777	5577	−2030	3.5
C(56)	3651 (3)	3988 (3)	1530 (12)	2.7 (2)′	H(66′)	3680	4861	−2207	3.5
C(57)	3222 (4)	3421 (4)	−1358 (9)	3.2 (3)′	H(66″)	3907	5128	−773	3.5
C(60)	2500	5122 (6)	−1848 (13)	2.6 (4)′	H(67)	3317	6195	1199	3.5
C(61)	3011 (4)	5268 (4)	−1074 (9)	2.5 (2)′	H(67′)	3579	5527	1402	3.5
C(62)	2823 (4)	5524 (4)	259 (10)	2.8 (3)′	H(67″)	3028	5738	2283	3.5
C(65)	2500	4866 (6)	−3390 (17)	3.9 (4)′					

motif is evident. The complicated packing is best seen by examination of Figure 1.

The four independent $[C(CN)_3]^-$ anions have approximate D_{3h} local symmetry.[26] The C–C bond lengths within experimental error are planar and vary from 1.367 (18) to 1.430 (10) Å and average 1.40 Å. The average C≡N bond length is 1.16 Å; however, individual r(C≡N)'s vary from 1.143 (10) to 1.192 (20) Å. These results are in good agreement with those determined in other $[C(CN)_3]^-$ salts[14-18] except that our value for r(C≡N) is slightly longer. There is a general difficulty in determining the distances for the $[C(CN)_3]^-$ to any degree of accuracy. For all of the structures examined, the errors in the C—C and C≡N distances are not negligible.[14-18]

Each crystallographically unique cation is essentially equivalent to each other and to the other $[Fe(C_5Me_5)_2]^{+\cdot}$'s previously

---

(26) The $[C(CN)_3]^-$ anions are labeled by the central carbon atom label. Anions C_1 and $C_{1''}$ are exactly planar. Anion $C_{1'}$ has a maximum deviation of 0.018 Å ($N_{1'}$) from the best plane. The largest deviation for anion $C_{3'}$ is 0.077 Å ($N_{1'}$) and the anion is slightly folded.

Table III. Interatomic Distances for $[Fe(C_5Me_5)_2]^{+}\cdot[C(CN)_3]^{-}$ (Å)

Fe(1)–C(10)	2.074 (7)	C(11)–C(12)	1.451 (13)
Fe(1)–C(11)	2.095 (7)	C(11)–C(16)	1.495 (12)
Fe(1)–C(12)	2.105 (8)	C(12)–C(13)	1.426 (11)
Fe(1)–C(13)	2.097 (8)	C(12)–C(17)	1.468 (12)
Fe(1)–C(14)	2.091 (7)	C(13)–C(14)	1.400 (10)
Fe(1)–C(20)	2.072 (7)	C(13)–C(18)	1.484 (11)
Fe(1)–C(21)	2.087 (8)	C(14)–C(19)	1.505 (11)
Fe(1)–C(22)	2.113 (7)	C(20)–C(21)	1.434 (10)
Fe(1)–C(23)	2.117 (8)	C(20)–C(24)	1.436 (10)
Fe(1)–C(24)	2.101 (7)	C(20)–C(25)	1.494 (10)
Fe(2)–C(30)	2.072 (13)	C(21)–C(22)	1.429 (9)
Fe(2)–C(31)	2.081 (9)	C(21)–C(26)	1.508 (11)
Fe(2)–C(32)	2.084 (10)	C(22)–C(23)	1.418 (10)
Fe(2)–C(40)	2.098 (12)	C(22)–C(27)	1.500 (10)
Fe(2)–C(41)	2.091 (8)	C(23)–C(24)	1.433 (10)
Fe(2)–C(42)	2.090 (9)	C(23)–C(28)	1.503 (9)
Fe(3)–C(50)	2.094 (11)	C(24)–C(29)	1.482 (11)
Fe(3)–C(51)	2.097 (8)	C(30)–C(31)	1.393 (11)
Fe(3)–C(52)	2.107 (8)	C(30)–C(35)	1.526 (20)
Fe(3)–C(60)	2.073 (12)	C(31)–C(32)	1.425 (14)
Fe(3)–C(61)	2.094 (8)	C(31)–C(36)	1.522 (12)
Fe(3)–C(62)	2.115 (8)	C(32)–C(32)[a]	1.407 (16)
N(2‘)–C(2‘)	1.150 (15)	C(32)–C(37)	1.511 (14)
N(2)–C(2)	1.169 (17)	C(40)–C(41)	1.437 (11)
N(2′)–C(2′)	1.192 (20)	C(40)–C(45)	1.476 (19)
N(2″)–C(2″)	1.147 (21)	C(41)–C(42)	1.448 (13)
N(3‘)–C(3‘)	1.168 (10)	C(41)–C(46)	1.489 (12)
N(3)–C(3)	1.143 (10)	C(42)–C(42)[a]	1.416 (16)
N(3′)–C(3′)	1.162 (10)	C(42)–C(47)	1.481 (13)
N(3″)–C(3″)	1.150 (11)	C(50)–C(51)	1.425 (10)
C(1‘)–C(2‘)	1.367 (18)	C(50)–C(55)	1.475 (16)
C(1‘)–C(3‘)	1.399 (10)	C(51)–C(52)	1.423 (10)
C(1)–C(2)	1.423 (17)	C(51)–C(56)	1.500 (10)
C(1)–C(3)	1.430 (10)	C(52)–C(52)[a]	1.402 (13)
C(1′)–C(2′)	1.380 (20)	C(52)–C(57)	1.501 (11)
C(1′)–C(3′)	1.393 (11)	C(60)–C(61)	1.392 (10)
C(1″)–C(2″)	1.407 (21)	C(60)–C(65)	1.552 (17)
C(1″)–C(3″)	1.404 (11)	C(61)–C(62)	1.432 (12)
C(10)–C(11)	1.426 (11)	C(61)–C(66)	1.511 (12)
C(10)–C(14)	1.422 (11)	C(62)–C(62)[a]	1.444 (17)
C(10)–C(15)	1.491 (12)	C(62)–C(67)	1.494 (12)

[a] $^1/_2 - x, y, z$.

Table IV. Intramolecular Angles for $[Fe(C_5Me_5)_2]^{+}[C(CN)_3]^{-}$

N(2‘)–C(2‘)–C(1‘)	179 (2)	C(23)–C(22)–C(27)	127.1 (7)
N(2)–C(2)–C(1)	180 (4)	C(22)–C(23)–C(24)	108.2 (6)
N(2′)–C(2′)–C(1′)	178 (2)	C(22)–C(23)–C(28)	125.8 (7)
N(2″)–C(2″)–C(1″)	180 (2)	C(24)–C(23)–C(28)	125.9 (6)
N(3‘)–C(3‘)–C(1‘)	177 (1)	C(20)–C(24)–C(23)	107.8 (6)
N(3)–C(3)–C(1)	179.1 (8)	C(20)–C(24)–C(29)	126.8 (7)
N(3′)–C(3′)–C(1′)	179 (1)	C(23)–C(24)–C(29)	125.4 (6)
N(3″)–C(3″)–C(1″)	179 (1)	C(31)–C(30)–C(31)[a]	110 (1)
C(2‘)–C(1‘)–C(3‘)	120.2 (5)	C(31)–C(30)–C(35)	125.0 (6)
C(3‘)–C(1‘)–C(3‘)[a]	120 (1)	C(30)–C(31)–C(32)	107.1 (9)
C(2)–C(1)–C(3)	119.3 (6)	C(30)–C(31)–C(36)	127 (1)
C(3)–C(1)–C(3)[b]	121 (1)	C(32)–C(31)–C(36)	126.1 (9)
C(2′)–C(1′)–C(3′)	118.8 (7)	C(31)–C(32)–C(32)[a]	107.9 (5)
C(3′)–C(1′)–C(3′)[c]	122 (1)	C(31)–C(32)–C(37)	126.1 (8)
C(2″)–C(1″)–C(3″)	119.9 (6)	C(32)[a]–C(32)–C(37)	126.0 (6)
C(3″)–C(1″)–C(3″)[d]	120 (1)	C(41)–C(40)–C(41)[a]	108 (1)
C(11)–C(10)–C(14)	107.5 (8)	C(41)–C(40)–C(45)	126.1 (6)
C(11)–C(10)–C(15)	127.1 (8)	C(40)–C(41)–C(42)	108.0 (8)
C(14)–C(10)–C(15)	125.1 (8)	C(40)–C(41)–C(46)	126.4 (9)
C(10)–C(11)–C(12)	107.6 (7)	C(42)–C(41)–C(46)	125.6 (8)
C(10)–C(11)–C(16)	124.6 (9)	C(41)–C(42)–C(42)[a]	108.2 (5)
C(12)–C(11)–C(16)	127.9 (9)	C(41)–C(42)–C(47)	125.6 (8)
C(11)–C(12)–C(13)	107.1 (7)	C(42)[a]–C(42)–C(47)	126.2 (6)
C(11)–C(12)–C(17)	125.5 (9)	C(51)–C(50)–C(51)[a]	106.5 (9)
C(13)–C(12)–C(17)	127.3 (10)	C(51)–C(50)–C(55)	126.6 (5)
C(12)–C(13)–C(14)	108.5 (7)	C(50)–C(51)–C(52)	108.7 (7)
C(12)–C(13)–C(18)	124.3 (8)	C(50)–C(51)–C(56)	126.3 (8)
C(14)–C(13)–C(18)	127.0 (8)	C(52)–C(51)–C(56)	124.9 (8)
C(10)–C(14)–C(13)	109.3 (7)	C(51)–C(52)–C(52)[a]	108.0 (4)
C(10)–C(14)–C(19)	124.7 (8)	C(51)–C(52)–C(57)	124.3 (7)
C(13)–C(14)–C(19)	126.0 (8)	C(52)[a]–C(52)–C(57)	127.5 (4)
C(21)–C(20)–C(24)	107.7 (6)	C(61)–C(60)–C(61)[a]	111 (1)
C(21)–C(20)–C(25)	126.1 (8)	C(61)–C(60)–C(65)	124.7 (6)
C(24)–C(20)–C(25)	125.8 (7)	C(60)–C(61)–C(62)	107.6 (8)
C(20)–C(21)–C(22)	107.9 (7)	C(60)–C(61)–C(66)	126.3 (9)
C(20)–C(21)–C(26)	125.5 (7)	C(62)–C(61)–C(66)	126.0 (8)
C(22)–C(21)–C(26)	126.5 (7)	C(61)–C(62)–C(62)[a]	107.1 (5)
C(21)–C(22)–C(23)	108.4 (7)	C(61)–C(62)–C(67)	125.9 (8)
C(21)–C(22)–C(27)	124.5 (7)	C(62)[a]–C(62)–C(67)	126.9 (5)

[a] $^1/_2 - x, y, z$. [b] $1 - x, 1 - y, z$. [c] $^3/_2 - x, y, z$. [d] $1 - x, -y, z$.

characterized.[3-5] The cation exhibits D_{5d} local symmetry with Fe–C distances between 2.072 (7) and 2.117 (8) Å averaging 2.092 Å. The C–C bonds within the C_5 rings and the C–Me bonds range from 1.392 (10) to 1.451 (13) and 1.468 (12) to 1.552 (17) Å, respectively. The average value for r(C–C) and r(C–Me) is 1.423 Å and for C–Me 1.498 Å, respectively. The average Fe–C and ring C–C distances are longer than the corresponding averages for the parent $Fe(C_5Me_5)_2$ compounds, i.e., 2.050 (2) and 1.419 (2) Å, respectively. The average C–Me distance is essentially equivalent to the 1.500 Å reported for the parent Fe^{II} compound.[27]

Spectroscopic Studies

Vibrational Spectroscopy. The only ion of interest from a vibrational point of view is the $[C(CN)_3]^-$ anion. The infrared spectrum $[Fe(C_5Me_5)_2]^{+}\cdot[C(CN)_3]^{-}$ in both the solid and CH_2Cl_2 solution shows a sharp strong band at 2162 cm^{-1} and a very weak shoulder at ~2200 cm^{-1}. Both in the solid and in solution, a weak band is found at 1226 cm^{-1}. The IR spectrum of solid $[NBu_4]^+[C(CN)_3]^-$ has a strong sharp peak at 2158 cm^{-1} and a shoulder at ~2205 cm^{-1}. The IR spectrum of the $[PPN]^+$ complex in the solid shows a strong sharp peak at 2169 cm^{-1} and a shoulder near 2200 cm^{-1}; in solution, the strong peak is at 2162 cm^{-1}.

The solid-state Raman spectrum of $[NBu_4]^+[C(CN)_3]^-$ shows peaks at 2159 and 2196 cm^{-1}. For the $[PPN]^+$ derivative peaks at 2162 and 2207 cm^{-1} are observed for the solid. In solution the peaks are at 2160 and 2208 cm^{-1}. Polarization experiments show that the peak at 2160 cm^{-1} is depolarized and the peak at 2207 cm^{-1} is polarized. In the solid, a weak peak at ~640 cm^{-1} is also present. Attempts to obtain the Raman spectra of $[Fe(C_5Me_5)_2]^{+}\cdot[C(CN)_3]^{-}$ as a solid were thwarted by decomposition.

There have been a number of previous studies of the vibrational spectrum of $[C(CN)_3]^-$, usually as the K^+ salts.[11-13] On the basis of this previous work, the X-ray structures (our work and others[14-17]), and molecular orbital calculations, we assign the structure of the ion to the D_{3h} point group. We then assign the peak at ~2210 cm^{-1} to the symmetric CN stretch (A_1') and the peak at ~2160 cm^{-1} to the asymmetric CN stretch (E'). The peak at 1226 cm^{-1} can be assigned to the C–C asymmetric stretch (E') while the peak at 640 cm^{-1} can be assigned to the symmetric C–C stretch (A_1'). It is interesting to note that there is little effect of the counterion on the vibrational spectra of $[C(CN)_3]^-$ even though the ion sizes and thus the charge diffusivity vary greatly.

Electronic Absorption Spectra. The electronic absorption spectra are shown in Figure 3 for two different cations, $[NBu_4]^+$ and K^+. The electronic spectra of the $[Fe(C_5Me_5)_2]^{+}\cdot$ and $[PPN]^+$ derivatives are similar but are complicated by transitions involving the cation. The spectra have three features for wavelengths <50 000 cm^{-1}. The dominant feature occurs at 47 170 cm^{-1} (ϵ = 28 600 M^{-1} cm^{-1} for the $[NBu_4]^+$ complex). The next peak is found at ~42 550 cm^{-1} (ϵ = 1000 M^{-1} cm^{-1} for the $[NBu_4]^+$ complex). A weak shoulder is found at ~36 360 cm^{-1} (ϵ = 200 M^{-1} cm^{-1} for the $[NBu_4]^+$ complex). We discuss the assignment of these spectra based on our molecular orbital calculations below.

Mössbauer Spectra. The room-temperature ^{57}Fe Mössbauer spectrum of $[Fe(C_5Me_5)_2]^{+}\cdot[C(CN)_3]^{-}$ consists of a singlet with an isomer shift of +0.48 mm/s with respect to natural iron foil. At 1.83 °K the isomer shift is +0.49 mm/s. The half-width at half-height changes slightly going from room temperature (0.48 mm/s) to 1.83 °K (0.64 mm/s). These results are consistent with iron being in the Fe(III) state. The low-temperature data are substantially different from the zero-field Zeeman split spectra

---

(27) Freyberg, D. P.; Robbins, S. L.; Raymond, K. N.; Smart, J. D., *J. Am. Chem. Soc.* **1979**, *101*, 892.

Table V. Bond Distances in $[C(CN)_3]^-$ and $[C(CN)_3]^{+a}$

source	ref	space group	local symmetry	r(C—C)	r(C≡N)	comment
$[Fe(C_5Me_5)_2]^+\cdot[C(CN)_3]^-$	*b*	orthorhombic *Pma*2	D_{3h}	1.402	1.159	X-ray, av value
$Ag^+ [C(CN)_3]^-$	18	orthorhombic *I*2*cm*	C_{2v}	1.54 (9) 1.41 (7) × 2	1.10 (9) 1.16 (5) × 2	X-ray, central carbon above plane of nitrogens
$[NH_4]^+[C(CN)_3]^-$	17	monoclinic $P2_1/c$	D_{3h}	1.40 (1)	1.15 (1)	X-ray
$K^+[C(CN)_3]^-$	15	triclinic $P\bar{1}$		1.39 (2)	1.17 (1)	X-ray 0.025 Å; carbons are above plane of nitrogens
$K^+[C(CN)_3]^-$	14	triclinic $P\bar{1}$	D_{3h}	1.40	1.15	X-ray
$[Sn(CH_3)_3]^+[C(CN)_3]^-H_2O$	16	orthorhombic $P2_12_12_1$	D_{3h}	1.40 (3)	1.15 (1)	X-ray
$[C(CN)_3]^-$	*b*		D_{3h}	1.413	1.165	DZ+D_{C^-}
$[C(CN)_3]^-$	*b*		D_{3h}	1.399	1.149	3-21G
$[C(CN)_3]^+$	*b*		D_{3h}	1.403	1.159	DZ+D_{C^+}
$[C(CN)_3]^+$	*b*		D_{3h}	1.386	1.147	3-21G

[a] All bond distances in Å. [b] This work.

Table VI. Vibrational Frequencies for $[C(CN)_3]^-$ and $[C(CN)_3]^{+a}$

		$[C(CN)_3]^-$		$[C(CN)_3]^+$	
mode	symmetry (activity)	exptl[b]	calcd	calcd	exptl[b]
C≡N sym str	A_1' (R)	2222	2527	2541	2298
C≡N asym str	E′ (R, IR)	2170	2471	2449	2266
C—C asym str	E′ (R, IR)	1228–1250	1328	1363	
out-of-plane umbrella	A_2'' (IR)		838	943	855
in-plane C–C–C bend	E′ (R, IR)	610	726	692	
C–C sym str	A_1'(R)	658	676	697	
out-of-plane bend	E″ (R)	478	616	486	
in-plane bend	A_2' (inactive)		514	480	
out-of-plane bend	A_2'' (IR)		183	214	
in-plane bend	E′ (R, IR)	139, 162	174	170	143

[a] Frequencies in cm^{-1}. [b] Reference 12.

seen for the $[DDQ]^{-}\cdot$,[2,28a] $[TCNE]^{-}\cdot$,[2,4] and $[TCNQ]^{-}\cdot$[2,28b] salts of $[Fe(C_5Me_5)_2]^{+}\cdot$.

Molecular Orbital Calculations

Molecular Structure. Molecular orbital calculations were done either in D_{3h} or C_{3v} symmetry with the different basis sets. The first calculations utilized the DZ+D_C basis set. Since double-ζ basis sets are known to be biased toward planar structures for compounds such as NH_3[29] and we wished to demonstrate that the structure has D_{3h} rather than C_{3v} symmetry, we included polarization functions on the central carbon. The calculated structure for the anion at the DZ+D_C level for the D_{3h} structure is given in Table V. The CC and CN bond lengths show excellent agreement with the experimental values and are within 0.01 Å, which is less than the experimental error limits. The molecule was deformed so that the CN groups were out of the plane by 1°. The energy of this C_{3v} structure is higher than that of the D_{3h} structure and the direction of the gradient moves the C_{3v} structure back to a planar D_{3h} geometry.

Vibrational Spectrum. Since the structure is planar, we could employ the computationally more efficient 3-21G basis set for the vibrational calculations. The 3-21G basis set usually gives vibrational frequencies within 10–15% of the experimental values. The determination of the force field is the definitive theoretical proof that the structure of the ion has D_{3h} rather than the C_{2v} symmetry of the $[(CN)_2C{=}C{=}N]^-$ resonance form. The structure of the anion with the 3-21G basis set is given in Table V and is in reasonable agreement with the experimental and DZ+D_C calculated structures. The 3-21G bond lengths are somewhat shorter than the DZ+D_C values.[30] The vibrational frequencies with their symmetry labels and IR and Raman activity are given in Table VI and are compared with experimental values. The absence of any imaginary frequencies confirms the D_{3h} structure.

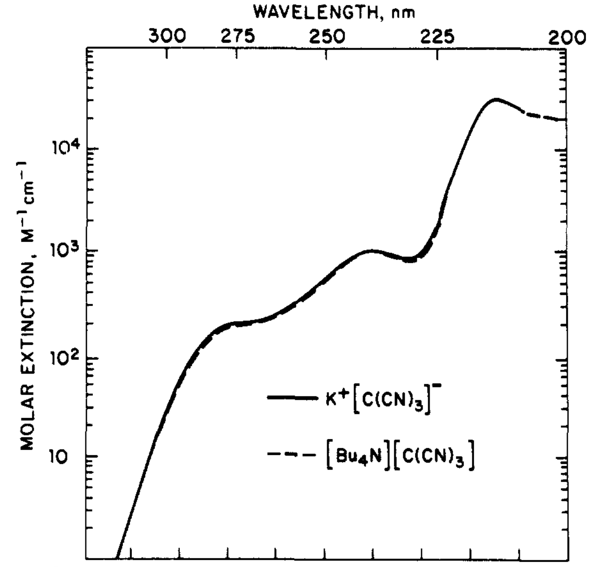

Figure 3. Electronic absorption spectra of $[C(CN)_3]^-$: (—) $K^+ [C(CN)_3]^-$, (- -) $[N(Bu)_4][C(CN)_3]$.

As expected, the vibrational frequencies are somewhat high compared to the experimental values. However, the ordering is in very good agreement. The theory predicts the symmetric C≡N stretch above the asymmetric C≡N stretch by almost the same amount as found experimentally. The asymmetric C–C stretch is significantly above the symmetric C–C stretch and confirms the assignment of the band near 1230–1250 cm^{-1} as being due to the asymmetric C–C stretch. The next transition is the A_2'' symmetric out of plane motion at 838 cm^{-1} which can be approximately described as the inversion bending mode. The next calculated bands are a degenerate in-plane bend at 726 cm^{-1} (E′) followed by the symmetric C–C stretch (A_1') at 676 cm^{-1}. The Raman spectrum of $K^+[C(CN)_3]^-$ shows a band at ~658 cm^{-1} which is polarized and a band at 610 cm^{-1} which is depolarized.[11-13] Furthermore, the band at 610 cm^{-1} can be observed in the IR.

---

(28) (a) Miller, J. S.; Krusic, P. J.; Reiff, W. M.; Zhang, J. H., manuscript in preparation; (b) Miller, J. S.; Preston, L. D.; Reis, J. H., Jr.; Gebert, E. Extine, M.; Troup, J.; Zhang, J. H.; Reiff, W. H., manuscript in preparation.

(29) Eades, R. A.; Weil, D. A.; Dixon, D. A.; Douglass, C. H., Jr. *J. Phys. Chem.* **1981**, *85*, 976.

(30) Such a result for the C–C bond could be expected based on a comparison of the geometries of CH_3CN at the 3-21G and 6-31G* levels. See ref 31.

Table VII. Summary of Results on High-Lying Occupied and Low-Lying Virtual Molecular Orbitals for the DZ+D_C-(+) Calculations

symmetry	eigenvalue (au)	comments
		$[C(CN)_3]^{-\,a}$
e′	−0.4080	in-plane
e″	−0.3421	C_N: 0.56 e^-; N: 0.77 e^-
e′	−0.3349	no population on C
a_2'	−0.3136	in-plane type, C_N: 0.30 e^-; N: 0.37 e^-
a_2''	−0.1563	HOMO, C: 1.10 e^-; N: 0.32 e
e′	0.3093	LUMO, large coefficient on C
e″	0.3380	
a_1'	0.4306	
		$[C(CN)_3]^{+\,b}$
e′	−0.8482	in plane
e′	−0.7806	C_N: 0.69 e^-; N: 0.64 e^-
a_2'	−0.7592	C_N: 0.29 e^-; N: 0.38 e^-
e″	−0.7463	HOMO, C_N: 0.76 e^-; N: 0.58 e^-
a_2''	−0.3534	LUMO, large coefficient on C(1)
e′	−0.1247	
e″	−0.0622	

[a] $E = -314.74517$ au. [b] $E = -314.23655$ au.

On the basis of symmetry, these bands are assigned as A_1' (658 cm^{-1}) and E′ (610 cm^{-1}). Thus the theory predicts a different order for these two bands. The out-of-plane bending E″ band is calculated at 616 cm^{-1} as compared to an experimental value of 478 cm^{-1}. The "invisible" A_2' bending mode is calculated to be at 514 cm^{-1}. There are two very low lying frequencies, an out-of-plane bend calculated at 183 cm^{-1} (A_2'') and an in-plane bend calculated at 174 cm^{-1} (E′). The E′ bend can be assigned to either the 139-cm^{-1} band observed by Beaumont et al.[12] or the 162-cm^{-1} band observed by Long et al.[13] The A_2'' band near 183 cm^{-1} has not been observed in the infrared.

Electronic Structure of $[C(CN)_3]^-$. Data on the molecular orbitals of the anion are summarized in Table VII. The highest occupied molecular orbital (HOMO) is at a much higher energy than the remaining orbitals. It is of a_2'' symmetry and is an out-of-plane π orbital. Although there is substantial population on C(1) (i.e., the central carbon), 1.10 e^-, the population on the nitrogens is 0.32 e^-; there is no population on the carbon, C_N. Application of Koopmann's theorem gives an estimate for the electron affinity of the $[C(CN)_3]\cdot$ radical of 4.25 eV. The next five occupied orbitals are close in energy and have the symmetries a_2', e′, and e″. Thus, the in-plane π orbitals (a_2', e′) are slightly higher in energy than the out-of-plane e″ π orbitals.

The LUMO is an in-plane orbital of e′ symmetry with a significant component on C(1). The next highest unoccupied MO is of e″ symmetry (out-of-plane π) with no coefficient on C(1). Thus, the first two electronic transitions are expected to be the $a_2''^2 \rightarrow a_2''e'$ and $a_2''^2 \rightarrow a_2''e''$, which have E″ and E′ symmetry, respectively. This is in agreement with an earlier extended Hückel calculation.[9] The transition $^1E' \leftarrow {}^1A_1'$ is allowed (second transition) while the HOMO → LUMO transition, $^1E'' \leftarrow {}^1A_1'$, is forbidden. We assign the large spectral feature at 47 200 cm^{-1} to the allowed transition following the previous assignment of Enemark and Holm.[9] The two other weaker features at 42 000 and 36 360 cm^{-1} are assigned to the forbidden HOMO → LUMO transition which is split. The lower wavelength peak is more intense because of borrowing from the strongly allowed band. The calculated energy difference in the two virtual orbitals is 0.78 eV (6300 cm^{-1}). If the transitions are governed by this energy difference then the forbidden transition would nominally be at 40 800 cm^{-1} if it is not split. However, the state should split by a Jahn–Teller distortion and give two peaks, one above and one below this value as is observed.

Charge Density of $[C(CN)_3]^-$. The Mulliken populations are given in Table VIII. A dominant amount of the out-of-plane charge is found at C(1) as expected. Furthermore, the out-of-plane C–N π orbital is polarized as $C^{\delta+}–N^{\delta-}$ whereas the in-plane C–N π orbital is polarized $C^{\delta-}–N^{\delta+}$ with p_Y populations at C of 1.07 e^- and at N of 1.00 e^-.

Table VIII. Population Analysis for $[C(CN)_3]^-$ and $[C(CN)_3]^+$ with the DZ+D_C Basis Set[a]

	$[C(CN)_3]^-$ pop.	$[C(CN)_3]^-$ p_z pop.	$[C(CN)_3]^+$ pop.	$[C(CN)_3]^+$ p_z pop.
C(1)	−0.21	1.61	0.41	0.51
C_N	−0.06	0.86	−0.03	1.11
N	−0.20	1.27	0.23	0.71

[a] Populations in electrons (e^-).

$[C(CN)_3]^+$. In order to better understand the bonding in the anion and to compare it with other cyano-substituted compounds, we have made a similar theoretical study of the tricyanocarbenium ion, $[C(CN)_3]^+$. The geometry was optimized at the DZ+D_C level and the bond distances are given in Table V. The bond distances decrease very slightly (~0.01 Å) from those in the anion. The C–C bond is slightly longer than that in H_2CCN^+. In contrast, the CN bond (1.159 Å) is somewhat shorter than that observed for $[C(CN)_3]^-$ and is slightly longer than that for MeCN (1.155 Å)[32] or calculated (1.125 and 1.139 Å).[33] This is in agreement with an averaging of the $[(CN)_2C{=}C{=}N]^+$ resonance forms which can contribute to this structure. The geometry for $[C(CN)_3]^+$ at the 3-21G level has shorter bond lengths than at the DZ+D_C consistent with the results for the $[C(CN)_3]^-$ structure.

The structure of the cation can be compared to the isoelectronic CH_3CN and $[H_2CCN]^+$. The C–C bond in $[C(CN)_3]^+$ is significantly shorter than that in CH_3CN (1.458 Å observed,[32] 1.468 Å 6-31G*,[31] 1.457 Å 3-21G).[31] The CN bond in $[C(CN)_3]^+$ is slightly lengthened from that in CH_3CN (1.155 Å experimental,[32] 1.135 Å 6-31G*,[31] 1.139 Å 3-21G).[31] This is consistent with the results for $^+CH_2CN$ where r(C–C) = 1.384 Å and r(C–N) = 1.165 Å with a DZ+P basis set.[33] The difference between $[CH_2CN]^+$ and CH_3CN has been explained in terms of an important contribution from the $[H_2C{=}C{=}N]^{+\,33}$ resonance structure. A similar argument can be made for $[C(CN)_3]^+$ in terms of the following three resonance strucures.

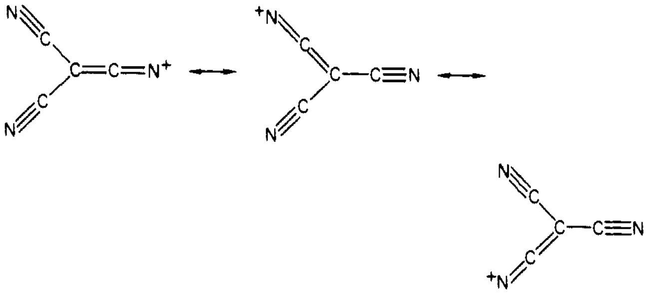

The similarity between the geometries of $[C(CN)_3]^+$ and $C(CN)_3^-$ suggests that the following resonance structures play an important role in the anion.

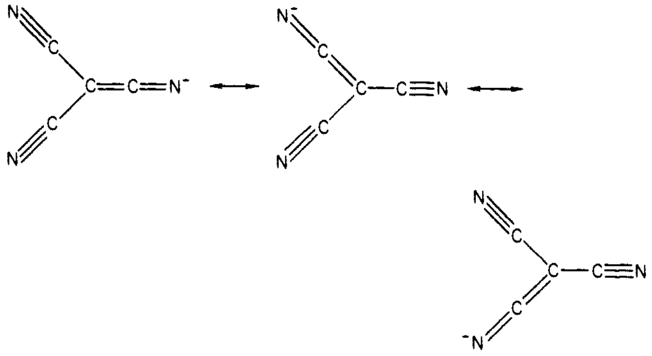

---

(31) Whiteside, R. A.; Binkley, J. S. Krishman, R.; DeFrees, D. J.; Schlegel, H. B.; Pople, J. A. *Carnegie-Mellon Quantum Chemistry Archive*, Carnegie-Mellon University, Pittsburgh, PA, 1980.

(32) Costain, C. C. *J. Chem. Phys.* **1958**, *29*, 864.

(33) (a) Dixon, D. A.; Charlier, P. A.; Gassman, P. G. *J. Am. Chem. Soc.* **1980**, *102*, 3957. (b) Dixon, D. A.; Eades, R. A.; Frey, R.; Gassman, P. G.; Hendewerk, M. L.; Paddon-Row, M. N.; Houk, K. N. *J. Am. Chem. Soc.* **1984**, *106*, 3885.

These structures are consistent with the shorter C–C bond and slightly longer C–N bond found in $[C(CN)_3]^-$ as compared to CH_3CN or to those in other R_3CCN compounds, e.g., for R = CN, $r(C—C) = 1.484$ Å and $r(C{\equiv}N) = 1.161$ Å.[34] They are also consistent with the planarity of the anion.

The calculated frequencies for the cation are given in Table VI and are quite similar to those for the anion. Essentially no change is found in the CN frequencies as compared to the anion. The C–C stretches are slightly higher in the cation than in the anion. The largest differences are found in the out-of-plane modes. The A_2'' mode at 943 cm^{-1} is $\sim$100 cm^{-1} higher in the cation than in the anion. This is consistent with the cation being harder to deform out-of-plane than the anion as is known for the case of simply substituted carbenium ions and carbanions. The E'' out-of-plane bend at 486 cm^{-1} in the cation is $\sim$120 cm^{-1} below that in the anion. Beaumont et al.[12] have studied the vibrational spectrum of the $[SbCl_5][ClC(CN)_3]$ adduct. If $[C(CN)_3]^+$ is present, we can assign the bands shown in Table VII as possibly being due to the cation; however, due to the difficulty in obtaining the experimental spectrum these assignments are only tentative.

The molecular orbitals for the cation differ somewhat from those in the anion. The HOMO is the out-of-plane π orbital of e'' symmetry and the next two orbitals are of a_2' and e' symmetry (in-plane π-type orbitals). The HOMO predicted from the anion would have a_2' symmetry, but this is clearly not the case for the cation. The LUMO for this system is of a_2'' symmetry and is clearly separated from the remaining virtual orbitals. The lowest lying electronic transitions for the cation will be from the top few occupied orbitals to the LUMO. In this case the HOMO → LUMO transition would be allowed.[35]

Comparison of the vibrational frequencies for $[C(CN)_3]^+$ and $[C(CN)_3]^-$ provides further insight into the structures of these compounds. The general conclusion reached from such a comparison is that the frequencies are quite similar. In terms of a valence bond argument this is consistent with the resonance forms for the anion contributing a comparable amount of those for the cation. One can also examine the molecular orbitals and reach a similar conclusion. The HOMO of the anion has essentially no density on C_N. There is no direct overlap between C(1) and N and removal of two electrons to form the cation should not significantly alter the bonding. Thus, little change in the frequencies would be expected.

The Mulliken populations are given in Table VIII for the cation. As in the case of the excess negative charge on the anion, the excess positive charge on the cation is found on the same atoms C(1) and N. Very little change in the charge is found on C_N in going from the anion to the cation. For the cation the CN out-of-plane π bond is polarized $C^{\delta-}–N^{\delta+}$. The CN in-plane bond is not polarized with p_Y populations of 1.01 e$^-$ on C_N and 1.03 e$^-$ on N. The out-of-plane populations on C(1), C_N, and N are similar to those found in the simpler compound[33] $[H_2CCN]^+$ where the populations are 0.25 e$^-$ on C(1), 1.13 e$^-$ on C_N, and 0.60 e$^-$ on N with a DZ+P basis set. Of course three resonance structures of the form $[R_2C{=}C{=}N]^+$ contribute to the compound with R = CN while only one contributes to the compound with R = H. Thus, the electron density on C(1) for R = CN will be larger than that for R = H. Since each resonance structure contributes less electron density on N, the electron density on N will be greater for R = CN than for R = H when only one resonance structure contributes.

Acknowledgment. We thank William M. Reiff and J. H. Zhang (Northeastern University) for obtaining the ^{57}Fe Mössbauer Spectra, B. Chase (duPont) for obtaining infrared and Raman spectra, and E. Mattews and R. E. Richardson (duPont) for obtaining electronic absorption spectra for $[Fe(C_5Me_5)_2]^+{\cdot}[C(CN)_3]^-$. We also thank R. M. Hilmer (duPont) for developing the digitization and complementary plotting software used in this research.

Registry No. $[Fe(C_5Me_5)_2]^+{\cdot}[C(CN)_3]^-$, 100021-50-9; $K[C(CN)_3]$, 34171-69-2; $[Fe(C_5Me_5)_2]^+{\cdot}[BF_4]^-$, 100021-51-0; $[PPN]^+{\cdot}[C(CN)_3]^-$, 100021-52-1; $[PPN]^+{\cdot}Cl^-$, 21050-13-5; $[n\text{-}Bu_4N]^+{\cdot}[C(CN)_3]^-$, 74908-12-6; $[n\text{-}Bu_4N]^+[BF_4]^-$, 429-42-5.

Supplementary Material Available: Complete listings of the anisotropic thermal parameters (Table II) and amplitudes and structure factors (10 pages). Ordering information is given on any current masthead page.

---

(34) Britton, D. *Acta Crystallogr.* **1974**, *B30*, 1818.

(35) An estimate of the ionization potential (IP) for $[C(CN)_3]\cdot$ can be made from the difference in energies between $[C(CN)_3]^-$ and $[C(CN)_3]^+$ and our estimate of the electron affinity of $[C(CN)_3]\cdot$.

Oxygenation of Styrene by Cytochrome P-450 Model Systems: A Mechanistic Study

James P. Collman,* Thomas Kodadek, and John I. Brauman

Contribution from the Department of Chemistry, Stanford University, Stanford, California 94305. *Received July 18, 1985*

Abstract: The manganese and iron porphyrin catalyzed oxygenation of styrene results in the production of phenylacetaldehyde as well as the expected epoxide. It is demonstrated that aldehyde is a primary product and does not result from isomerization of styrene oxide. Isotope labeling studies show that one of the β hydrogen atoms of styrene migrates to the benzylic carbon in the course of aldehyde formation. Experiments using cis and trans deuterated styrenes reveal that there is a stereoelectronic preference for migration of the hydrogen cis to the aromatic ring. Styrene, styrene-d_8, and *cis*-β-deuteriostyrene yield similar ratios of epoxide to aldehyde, indicating that β hydrogen migration occurs after the rate-determining step for formation of phenylacetaldehyde. The mechanism of this rearrangement is discussed. Some new information concerning the mechanism of olefin epoxidation by these catalysts is also presented. These results may have relevance to the mechanism of alkene oxygenation by the cytochrome P-450 monooxygenase enzymes.

Well-characterized examples of biological organometallic complexes are fairly rare, although many metalloenzymes catalyze reactions of organic substrates. It seems possible that some of these catalytic cycles involve as yet undetected metal–carbon bonded species as unstable intermediates. We have speculated that the cytochrome P-450's, an iron–heme based family of mo-

0002-7863/86/1508-2588$01.50/0